JOURNAL OF CATALYSIS 68, 270–285 (1981)

Characterization of Ni/TiO_2 Catalysts by TEM, X-Ray Diffraction, and Chemisorption Techniques

J. S. SMITH,* P. A. THROWER,† AND M. A. VANNICE*

*Department of Chemical Engineering and †Department of Materials Science & Engineering, The Pennsylvania State University, University Park, Pennsylvania 16802

Received June 26, 1980; revised October 27, 1980

Nickel crystallite sizes calculated from H_2, CO, and O_2 chemisorption are compared to those determined from X-ray diffraction (XRD) and transmission electron microscopy (TEM). Good agreement is obtained among all techniques for typical Ni/SiO_2 and Ni/Al_2O_3 catalysts, whereas sizes calculated from H_2 and CO chemisorption are far too large for Ni/TiO_2 catalysts. In contrast, oxygen chemisorption provides values in excellent agreement with those from XRD and TEM, and indicates that monolayer coverages of CO and H_2 are much lower on TiO_2-supported nickel. This agreement also implies that oxygen monolayer coverage on TiO_2-supported nickel does not exceed unity regardless of crystallite size, whereas coverages of two or higher are observed on SiO_2- and Al_2O_3-supported nickel, in agreement with previous studies. Isobars for CO and H_2 adsorption on Ni/TiO_2 clearly show that activated adsorption is not responsible for the low CO and H_2 uptakes at 300 K. Low-contrast nickel crystallites on titania are observed in the TEM micrographs, indicating that nickel may exist with a raft-like morphology on this support. These results provide evidence that strong metal–support interaction behavior exists in the Ni/TiO_2 system.

INTRODUCTION

Supported metal catalysts play an integral role in many industrial processes. Most of the metals of importance in catalysis are very expensive and maximum utilization is obtained by dispersing the metal on a porous, high-surface-area material, thereby creating very small crystallites and increasing the specific metal surface area. The support also inhibits sintering of the metal particles, a process which decreases the surface area. Although the support is frequently an inert material and is considered to have little effect on the catalytic properties of the metal in contact with its surface, a recent study by Tauster and co-workers (*1*) showed that strong metal–support interaction (SMSI) behavior can exist for Group VIII noble metals supported on TiO_2. Their study was primarily focused on the chemisorptive properties of the catalysts, and they found that CO and H_2 chemisorption was severely inhibited when the catalysts were reduced at 773 K while a reduction at 473 K led to normal chemisorption behavior. Their conclusion that a strong metal–support interaction existed in these systems was supported by Baker *et al.* (*2, 3*), who found very thin, raft-like Pt particles on a titania film when examined by transmission electron microscopy.

Altered adsorption behavior has been observed for all the Group VIII metals on TiO_2, and in most cases significant changes occurred in catalytic properties for CO hydrogenation (*4*). Titania-supported nickel exhibits some of the most apparent improvements in catalytic behavior, and Vannice and Garten (*5*) recently reported that both catalytic activity and selectivity toward higher hydrocarbon production in CO hydrogenation are much higher with titania-supported Ni catalysts than with conventional supported nickel catalysts. However, they observed that CO and H_2 adsorption was very low on Ni/TiO_2 when compared to typical nickel catalysts, and Ni particle sizes on TiO_2 calculated from H_2 and CO chemisorption were much larger than those

0021-9517/81/040270-16$02.00/0

indicated by X-ray line broadening results.

This study was undertaken to help clarify this disparity in calculated particle sizes, to see if decreased monolayer coverages of hydrogen and CO could be verified, and to determine if additional information could be obtained which would indicate the existence of SMSI behavior in Ni/TiO_2 catalysts. Toward this goal, transmission electron microscopy (TEM), X-ray diffraction measurements (XRD), and CO, H_2, and O_2 chemisorption were used to thoroughly characterize the catalysts, and crystallite sizes were calculated from all three techniques. For comparison, Ni/SiO_2 and Ni/Al_2O_3 catalysts were also prepared and characterized. Because nickel is more difficult to reduce than the noble metals, its transition to SMSI behavior is more difficult to observe, and a higher degree of characterization is required to verify this state (*5*).

EXPERIMENTAL METHODS

Materials

The support materials used in this study were SiO_2 (Grade 57) from Davison Chemical Company, TiO_2 (P-25) from Degussa Company, and η-Al_2O_3 from Exxon Research & Engineering Company. The SiO_2 pellets, with a reported surface area of 300 m^2 g^{-1}, were ground with a mortar and pestle and the 40/80-mesh fraction was used for catalyst preparation. The properties of the titania and η-alumina have been described elsewhere (*1*, *6*). All supports were dried in air for 20 hr at 465–483 K before use.

Ultrapure nickel hexahydrate, $Ni(NO_3)_2 \cdot 6H_2O$ (Alfa Corp.), was used as the metal salt in the catalyst preparations. All catalysts were prepared by an incipient wetness technique, and the required amounts of solution to fill the pore volumes were 0.4 ml g^{-1} for TiO_2, 0.5 ml g^{-1} for η-Al_2O_3, and 1.4 ml g^{-1} for SiO_2 (*7*). The impregnated catalysts were then oven-dried in air for 20 hr at 463–483 K, bottled, and stored in a desiccator. Weight loadings of the fresh unreduced nickel catalysts were determined by neutron activation analysis by comparison to a standard solution of nickel nitrate hexahydrate. The samples prepared included four Ni/TiO_2 catalysts with loadings of 1.4, 7.0, 8.6, and 12.3 wt%, 6.8% Ni/SiO_2, and 6.5% Ni/η-Al_2O_3, based on the unreduced catalyst.

Ultrahigh-purity hydrogen (99.9999%; Matheson Corp.) was further purified by passing it through a Deoxo purifier (Engelhard Ind.), an activated alumina trap, and an Oxy-trap (Alltech Assoc.) before it was used in chemisorption measurements. Before use, carbon monoxide (99.99% purity; Matheson) was passed through a molecular sieve trap to remove any carbonyls. Helium (99.9999% purity; Matheson) was flowed through an alumina trap and an Oxy-trap before use. The oxygen (99.99% purity from Linde or 99.994% purity from Air Products and Chemicals) was further purified by flowing it through a dry ice–acetone trap before it was used for chemisorption.

Apparatus and Procedure

Chemisorption

Adsorption measurements were performed in a conventional, mercury-free, glass vacuum system capable of achieving a dynamic vacuum of approximately 4×10^{7} Torr. Pressures were read from a Texas Instrument Precision Pressure Gage utilizing a quartz spiral Bourdon tube. A more detailed description of the adsorption unit is given elsewhere (*7*).

Catalyst samples of approximately 0.5 g were placed in a Pyrex adsorption cell and reduced *in situ* using hydrogen at a flow rate of 60 cm^3 min^{-1}. The stepwise pretreatment procedure for all catalyst samples was the high-temperature reduction procedure used by Tauster *et al.* (*1*). Typical manifold pressure at the end of the pretreatment was 3×10^{-5} Torr as measured by a Granville–

Phillips ionization gauge. The sequence in the chemisorption experiments was: (a) H_2 chemisorption; (b) determination of He dead volume; (c) reduction pretreatment; (d) CO chemisorption; (e) reduction pretreatment; (f) O_2 chemisorption.

The chemisorption of hydrogen on pure TiO_2 after this pretreatment was found to be zero, and hydrogen chemisorption on η-Al_2O_3 and SiO_2 has already been shown to be zero (*7, 8*). The room-temperature adsorption isotherms for oxygen on pure TiO_2, pure η-Al_2O_3, and pure SiO_2 were measured and the irreversible O_2 uptakes were determined by extrapolation to zero pressure (*9*). The isotherms for hydrogen and oxygen on the supported nickel catalysts and on the pure supports were found to be linear and essentially parallel at pressures above 50 Torr so the method of Benson and Boudart (*9*) and Wilson and Hall (*10*) was used to measure H_2 and O_2 uptakes. Because CO can exhibit considerable irreversible adsorption on pure support materials, the technique of Yates and Sinfelt (*11*) was used to measure CO chemisorption. This method utilizes two CO isotherms and the difference between the two isotherms at a pressure of 10 cm Hg (13.3 kPa) is used to represent the irreversible adsorption of CO on the nickel surface.

Each isotherm consisted of six data points typically covering a pressure range of 50 to 250 Torr. In all cases, 30 min was allowed for equilibration of the initial data point near 50 Torr. Little or no variation in the pressure was observed after this interval and provided justification for this time period. For the hydrogen chemisorption measurements the remaining five data points were obtained by allowing 2 min for equilibration to occur after each pressure increase. For the last 5 points in the O_2 isotherms and the last 11 points in the two CO isotherms, 5 min was allowed for equilibration before the pressure reading was taken. There was essentially no drift in the pressure readings taken during the hydrogen chemisorption measurements. A more detectable drift occurred during O_2 chemisorption, and during CO uptake measurements the drift in pressure was quite noticeable at times for the Ni/SiO_2 and Ni/Al_2O_3 catalysts, but was less noticeable for the Ni/TiO_2 catalysts. Titania is known to inhibit carbonyl formation (*5*), and this process is not considered a serious problem in the Ni/TiO_2 systems.

The percentage reduction of the nickel salt to metallic nickel in each supported catalyst was determined from the oxygen uptake at 698 ± 5 K following the procedure of Bartholomew and Farrauto (*12*). The O_2 uptake at 698 K on pure TiO_2 was 12.1 μmole g^{-1} and the total O_2 uptakes on the Ni/TiO_2 catalysts were corrected for this value.

Nickel dispersion, D (fraction exposed), was calculated based only on the amount of nickel reducible to metallic nickel; that is, the amount of unreducible nickel was assumed to interact so strongly with the support that it would not be part of the metal particles, and it was not considered when calculating metal dispersions and crystallite sizes. In determining the reduced nickel surface area, a cross-sectional area of 0.065 nm^2 was assumed for a nickel atom. This is calculated assuming equal areas exist for the (100), (110), and (111) crystallographic planes. Spherical particles were assumed to calculate average nickel particle sizes, and the final equation used was

$$\bar{d}_s \text{ (nm)} = 101/\%D, \qquad (1)$$

where $\bar{d}_s$ represents the surface-weighted average crystallite diameter and shows that particles less than 1 nm in size are 100% dispersed.

Hydrogen isobars at saturation pressures between 50 and 250 Torr were determined for the 7.0% Ni/TiO_2, 6.8% Ni/SiO_2, and 6.5% Ni/Al_2O_3 catalysts by measuring isotherms at room temperature, 373, 473, and 573 K, and plotting uptakes versus temperature. A CO isobar at 100 Torr was also obtained for the 7.0% Ni/TiO_2 catalyst.

X-Ray Diffraction

X-Ray line broadening experiments were performed on a Rigaku Geigerflex Model 4036-A1 diffractometer using Cu$K\alpha$ radiation with a graphite monochromator. A fast scan of 4° (2θ) min^{-1} was utilized for the 2θ range of 20 to 90°, while a slower scan of 1° (2θ) min^{-1} was carried out for 2θ from 42 to 55°. The slow scan encompassed the two major peaks, Ni(111) and Ni(200), and provided greater sensitivity for line broadening measurements. With the TiO_2- and Al_2O_3-supported catalysts there was an overlap of the Ni(111) peak and a particular peak of the support material, so for these cases the Ni(200) peak was used for line broadening calculations. All X-ray diffraction measurements were performed on samples that had been previously reduced and exposed to the atmosphere. The samples were packed into an aluminum holder backed by a glass slide.

Volume-weighted crystallite sizes were calculated from the X-ray diffraction measurements using the Scherrer equation,

$$\bar{d}_v = K\lambda/\beta \cos\theta_B, \qquad (2)$$

where λ is the wavelength of the radiation, β the line broadening of the peak due to the small crystallites, and θ_B the corresponding angle of the diffraction peak. The typical value of 0.9 was used for K, the Scherrer constant. Breadths at half-height were measured and Warren's correction, $\beta^2 = B^2 - b^2$, was used to correct for instrumental broadening, where B is the total broadening and b the instrumental broadening. For the 2θ range of the slow scan, the instrumental broadening was previously measured to be $2\theta = 0.26°$ (*13*).

Transmission Electron Microscopy

The electron microscopy study was performed using a Philips EM 300 transmission electron microscope. In all cases, a 30-μm objective aperture was used to increase contrast between the metal particles and the support material. The objective lens used provided the capability to tilt the specimen, and this limited the magnification to ~200,000× and the resolution to 1–1.5 nm. Contamination of the specimen by breakdown of residual organic molecules in the column due to the electron beam was limited by a liquid-nitrogen anticontamination trap. The specimen chamber was cooled below 143 K by conduction through copper wires to a brass anticontamination chamber surrounding the specimen. All micrographs were taken at a magnification of 200,000× and enlarged to 500,000×. All nickel particle counts were carried out at the final magnification of 500,000×.

The samples for TEM were prepared by ultrasonic dispersion after the catalyst powder was ground and passed through a 100-mesh screen. A small amount of this catalyst powder (~2–10 mg) was added to 10 ml of toluene and dispersed for 30 min. The suspension was allowed to sit for approximately 30 sec to allow the larger support particles to settle out. One drop of the suspension was then placed on a carbon-coated copper grid, and the samples were dried naturally while exposed to the atmosphere.

Micrographs were taken for the 7.0 and 12.3% Ni/TiO_2 catalysts, the 6.8% Ni/SiO_2 catalyst, and the 6.5% Ni/Al_2O_3 catalyst. Due to the low nickel content of the 1.4% Ni/TiO_2 and similarity in weight loading of the 8.6 and 7.0% Ni/TiO_2 samples, TEM work was not carried out on 1.4 and 8.6% Ni/TiO_2. Micrographs of the pure support materials were taken for comparison. The majority of the Ni particles could be approximated as spherically shaped, and the diameters were determined in a straightforward manner. However, some of the particles on TiO_2 were of very low contrast with the support and appeared to be two-dimensional or "raft-like." These particle shapes were approximated as rectangles, and the mean of the lengths of the sides was taken to represent their particle sizes.

RESULTS

Chemisorption

All runs were repeated at least once on a different catalyst sample and Table 1 gives the results of the chemisorption studies. Very little irreversible CO and O_2 uptake occurred on the pure supports except for the oxygen taken up by pure TiO_2 (7.1 μmole g^{-1}). Initial CO and O_2 adsorption runs showed that high admission rates of gas to the catalyst sample could greatly increase observed uptakes, especially for O_2, as shown in Table 1. The high heats of adsorption for CO and O_2 on nickel at room temperature (CO ~ 35 kcal $mole^{-1}$, O_2 ~ 125 kcal $mole^{-1}$ (*14*)) could produce substantial temperature gradients in the catalyst if the initial gas introduction was too rapid. These temperature excursions could enhance bulk oxidation or facilitate nickel carbonyl formation when carbon monoxide is present, and the two anomalously high uptake values are attributed to this cause. Consequently, small aliquots of CO and O_2 were admitted to the catalyst cell in a slow, stepwise manner which provided reproducible adsorption measurements. Hydrogen uptakes were not sensitive to admission rates. A thorough error analysis showed that the maximum error in the chemisorption experiments was ± 0.5 μmole.

Figure 1 depicts typical isotherms for H_2, CO, and O_2 adsorption on a Ni/TiO_2 catalyst. After the initial 30-min equilibration period, the gas pressure readings for both

TABLE 1

Chemisorption and X-Ray Results for Nickel Catalysts

Catalyst	Percentage reduction[a]	Adsorption (μmole g^{-1})[b]			$\bar{d}_v$ from XRD (nm)	Sample No.
		H_2	CO	O_2		
1.4% Ni/TiO_2	86	5.0	34.9	25.3	ND[c]	1
		5.5	33.1	26.3	ND	2
7.0% Ni/TiO_2	89	20.7	248[d]	76.3	12	1
		20.5	53.7	76.5	9	2
		20.6	—	—	—	2
		23.0	58.8	80.0	8	3
		22.5	54.2	—	—	4
8.6% Ni/TiO_2	94	30.5	84.4	119	8	1
		31.2	87.5	120	12	2
12.3% Ni/TiO_2	89	45.2	91.4	645[d]	9	1
		46.9	77.0	202	8	2
		48.0	—	186	—	3
		44.0	—	178	—	3
6.5% Ni/Al_2O_3	83	80.0	165	186	ND	1
		—	—	191	—	1
		80.0	—	211	8	2
		—	—	247	—	3
6.8% Ni/SiO_2	100	98.2	184	196	10	1
		105	—	—	—	2
Pure TiO_2		~0	~0	7.1		
Pure η-Al_2O_3		0[e]	1.0	0.5		
Pure SiO_2		0[e]	0.7	0.3		

[a] Corrected for 12.1 μmole g^{-1} O_2 uptake on pure TiO_2 at 698 K for TiO_2-supported catalysts.
[b] Total uptake before correction for irreversible adsorption on the support.
[c] ND, not detectable.
[d] Gas admission too rapid.
[e] Ref. (*7*).

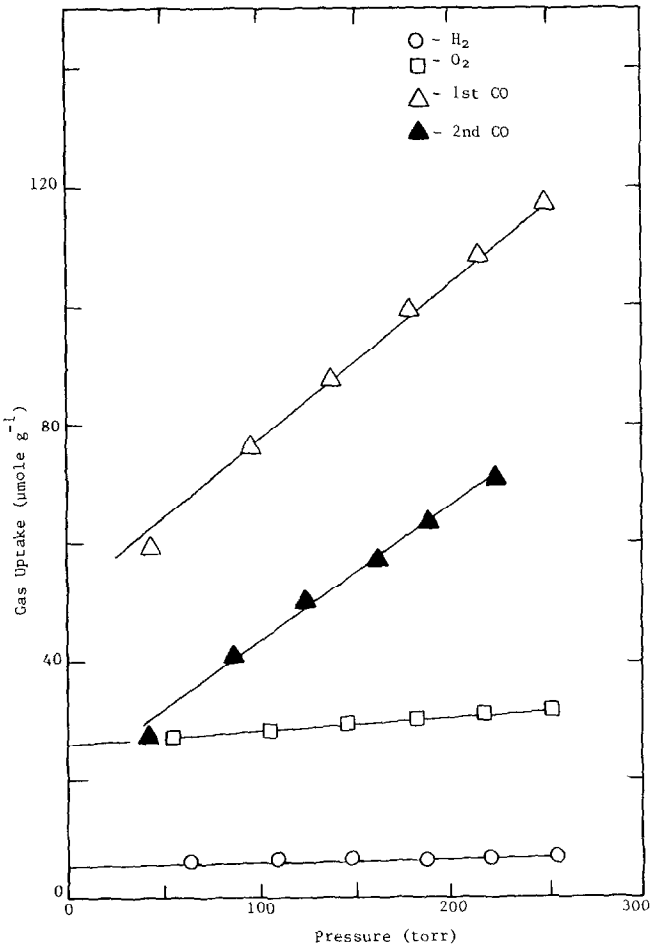

FIG. 1. Adsorption on 8.6% Ni/TiO_2 at 300 K.

H_2 and O_2 adsorption were essentially constant; however, the slow decline in the pressure observed during CO adsorption measurements is attributed to the formation of nonvolatile nickel subcarbonyls (*8*), because the use of titania as a support severely inhibits the rate of $Ni(CO)_4$ formation (*5*). Drifting in the CO pressure readings was more evident with Ni/SiO_2 and Ni/Al_2O_3 catalysts than with Ni/TiO_2 catalysts, which is consistent with previous results which showed that carbonyl formation can occur at 300 K with Ni/SiO_2 and Ni/Al_2O_3 catalysts (*5, 8*). Although some uncertainty may exist about the adsorption process, CO uptakes were in consistent agreement with H_2 uptakes, as shown in Table 2.

The percentage reductions of the nickel salt to nickel metal are given in Table 1. In all cases the percentage reductions, as determined by O_2 adsorption at 698 K, were quite high and consistent with values reported by Bartholomew *et al.* (*8, 12*). Although the irreversible O_2 uptake was measured for pure TiO_2, there is always the possibility that this value is low since noble metals can catalyze the reduction of TiO_2 to nonstoichiometric oxides which may adsorb more oxygen than TiO_2 (*2*). If nickel also catalyzes the reduction of TiO_2, then the oxygen uptakes by titania in the

TABLE 2

Average Adsorbate/Nickel Ratios for Supported Catalysts[a]

Catalyst	H/Ni_r	CO/Ni_r	O/Ni_r	CO/H	O/H	O/CO
1.5% Ni/TiO_2	—	—	—	4.7[b]	—	—
1.4% Ni/TiO_2	0.050	0.17	0.18	3.4	3.6	1.1
2.8% Ni/TiO_2	—	—	—	2.2[c]	—	—
7.0% Ni/TiO_2	0.041	0.053	0.13	1.3	3.2	2.5
8.6% Ni/TiO_2	0.045	0.063	0.16	1.4	3.6	2.6
10% Ni/TiO_2	—	—	—	1.4[b]	—	—
12.3% Ni/TiO_2	0.050	0.045	0.20	0.9	3.9	4.3
6.5% Ni/η-Al_2O_3	0.17	0.18	0.45	1.0	2.6	—
9% Ni/Al_2O_3	—	—	—	1.1[c]	—	—
6.8% Ni/SiO_2	0.18	0.16	0.34	0.9	1.9	—
13.5% Ni/SiO_2	0.41	—	—	1.1[c]	—	—

[a] Corrected for adsorption on support and based on amount of reducible Ni, Ni_r.
[b] Ref. (*5*).
[c] Ref. (*8*).

Ni/TiO_2 samples could be larger than the blank. However, the percentage reductions determined for Ni/TiO_2 are very consistent with the results for Ni/SiO_2 and Ni/Al_2O_3, which do not have this problem, and with other Ni/TiO_2 determinations (*15*).

Table 2 presents the average adsorbate/nickel ratios determined in this study, and shows that all the H/Ni_r and CO/Ni_r ratios for the TiO_2-supported catalysts were very low. Here Ni_r represents only the reduced nickel. Such low ratios are normally indicative of a poorly dispersed catalyst which contains large metal crystallites with a low surface to volume ratio. However, these ratios are quite similar to those reported by Tauster *et al.* (*1*) for the Group VIII noble metals supported on titania, and they verify the ratios reported previously by Vannice and Garten (*5*). *Oxygen chemisorption on titania-supported metals has not been reported, and this study is the first to examine the behavior of O_2 adsorption on TiO_2-supported nickel.* It is clear that O/Ni_r ratios are always significantly higher than H/Ni_r ratios. Since the H/Ni_s ratio, where Ni_s is a surface atom, is near unity for unsupported nickel and nickel on typical supports (*8, 15*), it is clear that either large Ni crystallites are prevalent in the Ni/TiO_2 catalysts or hydrogen monolayer coverages on TiO_2-supported nickel are significantly reduced.

The H/Ni_r and CO/Ni_r ratios determined for the SiO_2- and Al_2O_3-supported catalysts indicate no carbonyl formation, moderate dispersions, and H/CO ratios near unity, which are expected for dispersions in this range (*8*). The oxygen uptakes were clearly higher, with O/H ratios near 2 for Ni/SiO_2 and somewhat greater than 2 for Ni/Al_2O_3. Oxygen chemisorption on 6.5% Ni/Al_2O_3 was less well defined, and the irreversible uptake was more difficult to determine in some cases. Two O_2 isotherms for 6.5% Ni/Al_2O_3 were well-behaved, but two other O_2 isotherms were not linear and showed a rather steep rise at lower pressure before achieving a slope similar to the linear isotherms at higher pressures. The reason for this behavior is not clear, and for these latter two isotherms the O_2 uptake was determined by taking the difference at 300 Torr between the isotherms on alumina-supported nickel and pure alumina.

Hydrogen isobars were determined for the 6.8% Ni/SiO_2, 6.5% Ni/Al_2O_3, and 7.0% Ni/TiO_2 catalysts to ascertain if there was any evidence of activated adsorption. These isobars, which utilized the uptakes

from a zero-pressure extrapolation over a region of 100–250 Torr, are given in Fig. 2. The isobar for CO adsorption on 7.0% Ni/TiO_2, where CO uptakes were measured at 100 Torr, is also shown in Fig. 2.

XRD

X-Ray diffraction scans were performed on both the supported catalysts to determine nickel crystallite sizes and the pure support materials to establish baseline diffraction peaks. Calculated particle sizes are listed in Table 1.

TEM

Four catalysts—6.8% Ni/SiO_2, 6.5% Ni/Al_2O_3, 7.0% Ni/TiO_2, and 12.3% Ni/TiO_2—were studied using TEM to directly determine crystallite size distributions from which $\bar{d}_S$ and $\bar{d}_V$ values could be calculated and compared to those obtained from chemisorption and X-ray techniques. Flynn *et al.* (*16*) have shown that, in general, identical particles imaged in different micrographs can appear of different size because of differences in defocus. They also state that for analysis of size distribution, division of sizes into classes which differ by less than 1 nm is not warranted; therefore, the particle counts carried out in this study were separated into intervals of 1 nm.

As expected, the 6.8% Ni/SiO_2 catalyst was the easiest to characterize, and the Ni crystallites could readily be distinguished from the silica support even though the electron density of nickel is lower than that of the noble metals. Figure 3 shows a histogram based on a count of 298 particles. Ni/SiO_2 catalysts have been characterized previously in this manner (*17–19*), and the work reported here was done to provide an

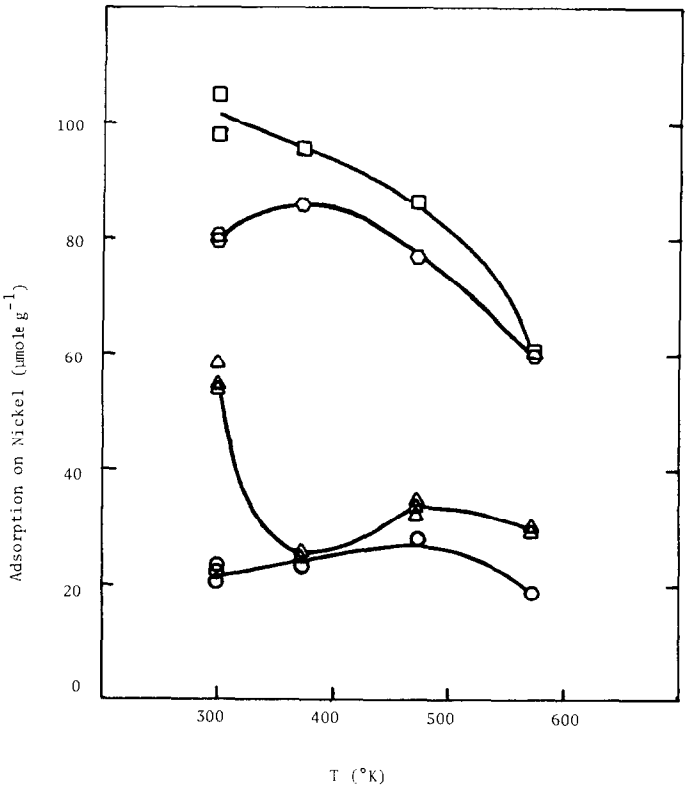

FIG. 2. Isobars for H_2 at 25 kPa and CO at 13 kPa on supported nickel. (□) H_2 on 6.8% Ni/SiO_2; (○) H_2 on 6.5% Ni/μ-Al_2O_3; (○) H_2 on 7.0% Ni/TiO_2; (△) CO on 7.0% Ni/TiO_2.

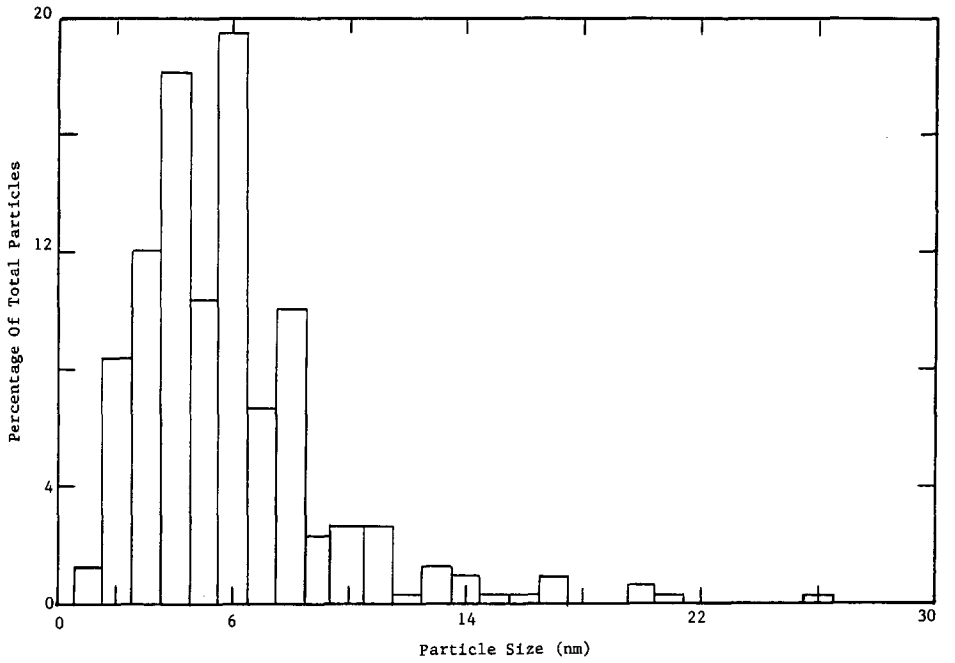

FIG. 3. Nickel particle size distribution on 6.8% Ni/SiO_2.

internal basis of comparison for the titania-supported nickel.

A problem existed with the TEM characterization of the 6.5% Ni/Al_2O_3 because the grainy (or spongy) appearance of the η-alumina made it much more difficult to distinguish nickel particles from the support material. Due to this lack of contrast between support and nickel particles, no meaningful particle size distribution could be determined. This situation is identical to that encountered in the studies of Mustard and Bartholomew (*15*) and Shephard (*20*).

The study of the titania-supported nickel samples by TEM posed some unique and rather difficult problems. Figure 4 is a micrograph of pure TiO_2 and reveals the variation in thickness between different regions in the pure TiO_2 samples. This lack of transparency results primarily from the crystalline nature of the TiO_2 particles which leads to a relatively large degree of diffraction contrast. Figure 4 also clearly indicates that darkened areas occur as a consequence of increased absorption due to the overlap of two or more titania crystals. Attention was focused on the relatively transparent areas of the titania, such as regions near the edges of particles, which facilitated the distinction between nickel particles and the support. As Fig. 4 shows, the transparent regions of the pure TiO_2 show no evidence of small crystallites. When the Ni/TiO_2 catalysts were examined by TEM, though, these transparent regions revealed a considerable number of Ni particles, as shown in Fig. 5 for the 7.0% Ni/TiO_2 catalyst. Histograms for both 7.0 and 12.3% Ni/TiO_2, based on particle counts of 111 and 127, respectively, were very similar (*21*). The histogram for 12.3% Ni/TiO_2 is shown in Fig. 6. The greater error involved in the smaller particle counts is recognized, but the restriction of locating nickel particles in transparent regions limited the number of particles which could be counted. However, many different areas from many different catalyst particles were examined to obtain the given particle count so that the shapes of the histograms should be statistically significant.

The most difficult part of the TEM inves-

FIG. 4. Electron micrograph of pure TiO_2. Scale = 10 nm.

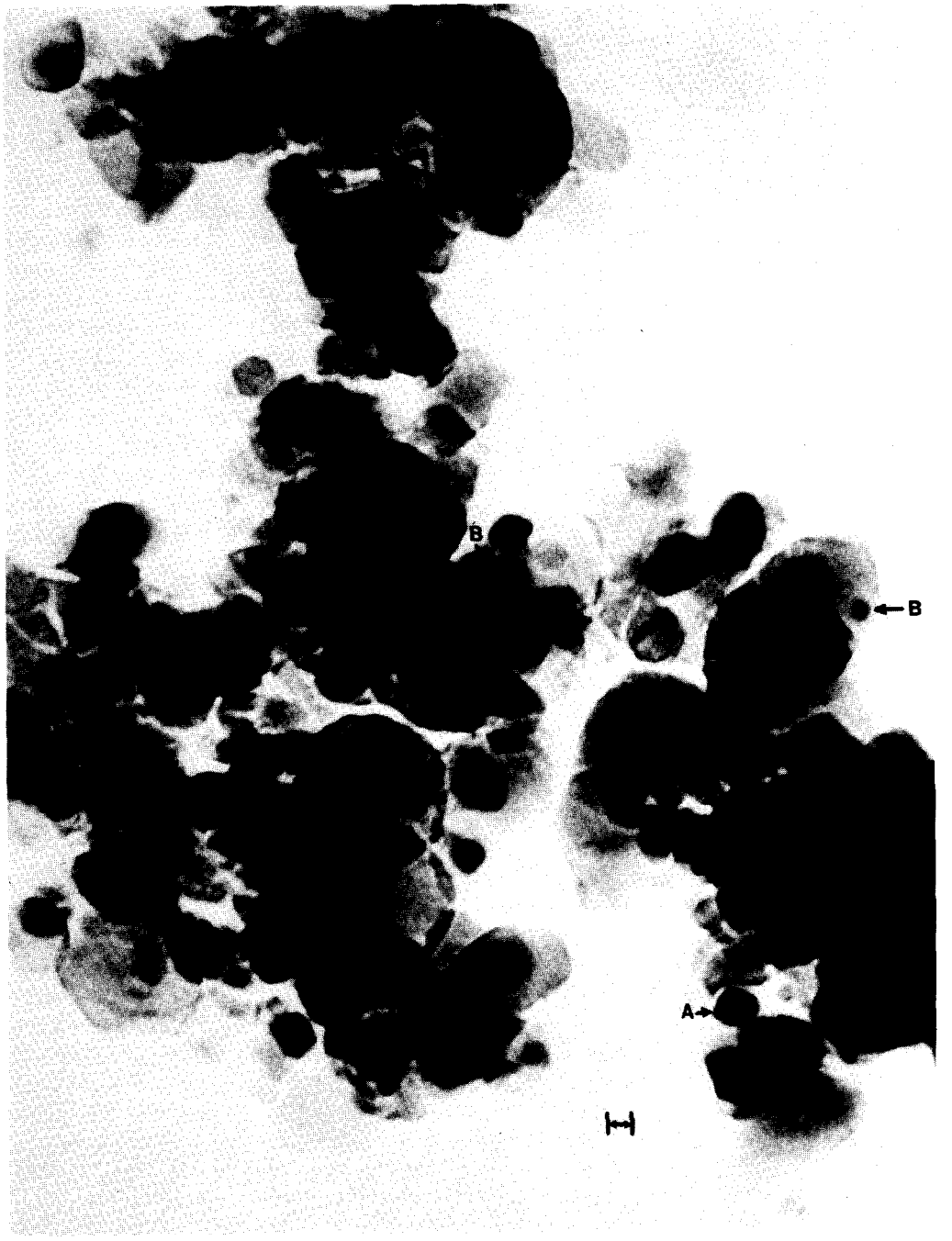

FIG. 5. Electron micrograph of 7.0% Ni/TiO_2. A denotes a "three-dimensional" (high contrast) particle; B denotes a "raft-like" (low contrast) particle. Scale = 10 nm.

tigations of the TiO_2-supported catalysts was the differentiation of the nickel particles from the TiO_2 support as indicated by a comparison of Figs. 4 and 5. A related consideration are the recent studies by Baker *et al.* (*2, 3*) of two-dimensional, "pill-box"

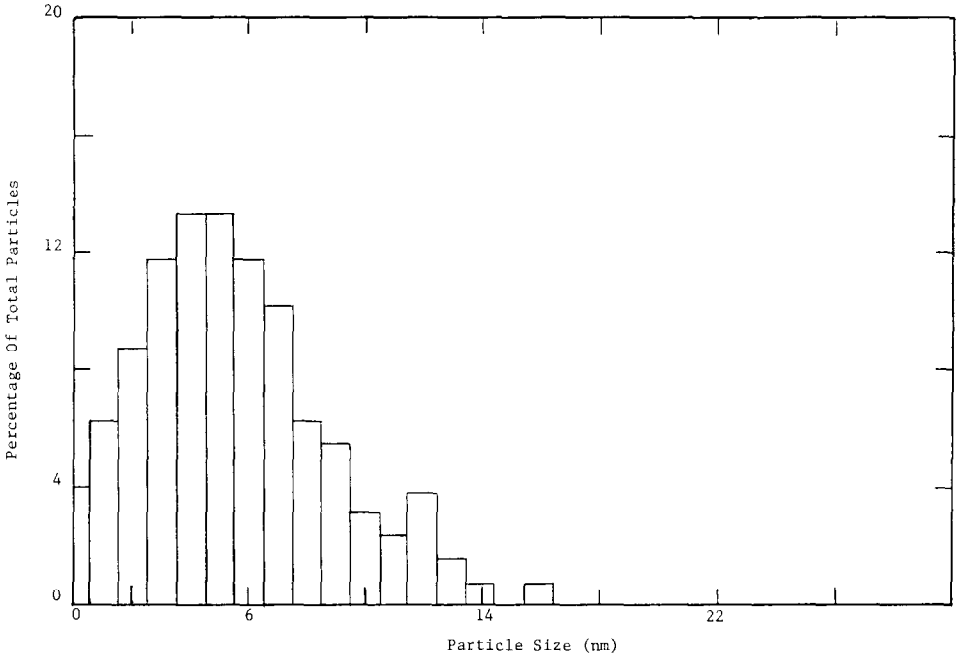

FIG. 6. Nickel particle size distribution on 12.3% Ni/TiO_2.

particles of Pt on a titania surface. Metal particles possessing a thin, raft-like morphology have also been detected in silica-supported catalysts (*22, 23*). Rather than appearing as very dark regions typical of three-dimensional Pt particles, which have a high electron density, the majority of the particles showed low contrast with the support material, thereby leading Baker *et al.* (*2, 3*) to the conclusion that raft-like particles exist. The lack of contrast is amplified in this study because nickel has a lower electron density than Pt, and Fig. 5 reveals many circular metal particles of low contrast, thereby indicating that thin, raft-like metal structures may possibly exist in Ni/TiO_2 catalysts. Nickel particles with this morphology have recently been proposed by Mustard and Bartholomew (*15*). The presence of both three-dimensional particles (high contrast) and raft-like particles (low contrast) seems to be indicated by the micrograph, and both forms have been depicted in Fig. 5. Many micrographs of all four catalyst systems have been reported elsewhere (*21*).

In many cases it was very difficult to decide whether a particle should be classified as a raft-like or a three-dimensional crystallite, and this assignment was at times quite subjective. Due both to this problem and to the relatively few particles counted, all morphologies were included in the histograms. Although the low contrast shown in Fig. 5 is not absolute proof of such two-dimensional crystallites (*24*), it does indicate that titania may have a significant effect on the morphology of supported Ni particles.

From the actual distributions determined by TEM, surface-weighted ($\bar{d}_S$) and volume-weighted ($\bar{d}_S$) averages can be calculated and compared to those determined by chemisorption and X-ray measurements (*25*). These values are listed in Table 3. The agreement among techniques is considered satisfactory for Ni/SiO_2 and Ni/Al_2O_3 and is comparable to results in the literature (*15, 17, 18*). For Ni/TiO_2, agreement among TEM, XRD, and O_2 chemisorption is excellent for 7.0% Ni/TiO_2 and very good for 12.3% Ni/TiO_2. The larger crystal-

TABLE 3

Average Nickel Particle Sizes

Catalyst	$\bar{d}_s$ (nm)					$\bar{d}_v$ (nm)	
	H_2	CO	O_2		TEM[a]	XRD	TEM[a]
			b	*c*			
7.0% Ni/TiO_2	25	19	8	16	8	10	9
12.3% Ni/TiO_2	20	22	5	10	9	8	10
6.8% Ni/SiO_2	6	6	3	6	11	10	14
6.5% Ni/η-Al_2O_3	6	6	2	5	—	10	—

[a] All TEM results are mean values.
[b] Assuming $O/Ni_s = 1$.
[c] Assuming $O/Ni_s = 2$.

lite sizes calculated from H_2 and CO adsorption have been reported before (*5, 15*), and clearly do not agree with other values for TiO_2-supported nickel.

DISCUSSION

Titania-supported nickel catalysts have exhibited unusually high activity for CO hydrogenation and a pronounced shift in selectivity to higher-molecular-weight hydrocarbons (*5, 26*). In addition, distinct changes occurred in the chemisorption of CO and H_2, and saturation coverages at 300 K appeared to be significantly lower than on typical nickel surfaces. A major aspect of this study was a more complete investigation of the adsorption properties of Ni/TiO_2 catalysts, including oxygen adsorption, over a wider range of nickel loadings than previously reported.

The chemisorption properties of the Ni/SiO_2 and Ni/Al_2O_3 catalysts were very consistent with previous results, as shown in Table 2. The CO/H ratios were near unity, which is expected for these catalysts at this weight loading and percent reduction in the absence of carbonyl formation (*8*). Also, at dispersions below 20%, as determined by the H/Ni_T ratios, O/Ni_T ratios near 2 would be expected from the correlation of Criado (*27*) for Ni/SiO_2 catalysts, and from many previous studies of oxygen adsorption on unsupported nickel (*18, 28–33*). Criado (*27*) has reported that the O/H adsorption ratio increases linearly from unity to 2 as nickel dispersion varies from 100% to values below ~20%. Under certain conditions, even higher O/Ni_T ratios have been observed which may be indicative of bulk oxide formation (*33, 34*). The 6.8% Ni/SiO_2 catalyst fits Criado's plot precisely while the Ni/Al_2O_3 catalyst produced O/H ratios somewhat higher than predicted. With these catalysts, especially Ni/SiO_2, good agreement was found between particle sizes calculated from H_2, O_2, and CO uptakes if the oxygen adsorption stoichiometry predicted by Criado's correlation, i.e., 2, was used.

The adsorption properties of the Ni/TiO_2 catalysts are noticeably different, especially regarding the O/H adsorption ratio. This ratio was always higher than those obtained for other nickel catalysts, and usually was near 4. The CO/H ratio was near 4 at low loadings but declined to unity at high loadings. It is important to note that adsorption of hydrogen, which is usually considered the best adsorbate for nickel surface area measurements (*8*), appears to be more inhibited than either CO or O_2 adsorption. As a consequence, H_2 adsorption is not a satisfactory technique to measure nickel dispersions on titania (*5, 15*), and may not be applicable to nickel on any SMSI support. This reduced hydrogen ad-

sorption capacity could account for the enhanced chain-growth observed over Ni/TiO_2 catalysts because the hydrogenation activity would be expected to be lower compared to typical nickel catalysts (*26*).

The large discrepancy between particle sizes estimated from CO and H_2 chemisorption is clearly shown in Table 3. The excellent agreement between the $\bar{d}_v$ values from XRD and TEM strongly implies that these results are the more accurate, and the recent study by Mustard and Bartholomew (*15*) also supports this conclusion. From comparison of the various techniques, it seems obvious that saturation coverages of CO and H_2 on TiO_2-supported nickel surfaces are much lower than coverages on typical nickel surfaces.

Oxygen adsorption measurements surprisingly appear to be the most accurate chemisorption technique for determining nickel crystallite size in Ni/TiO_2 systems. For Ni/SiO_2 and Ni/Al_2O_3 catalysts, crystallite size estimates from all three chemisorption techniques are in excellent agreement if Criado's relationship is used, as shown in Table 3. The assumption of an O/Ni_s adsorption ratio of unity for these two catalysts clearly results in much poorer agreement; however, for the TiO_2-supported nickel best agreement is obtained among O_2 adsorption, XRD, and TEM by assuming an O/Ni_s ratio of 1. This stoichiometry is unusual because it has previously been found to apply only to very small nickel crystallites (*27*).

The assumption of $O/Ni_s = 2$ gives sizes that are too large, especially for 7.0% Ni/TiO_2. The choice of $O/Ni_s = 1$ is preferred because adsorption techniques are sensitive to all crystallite surfaces whereas very small Ni particles will not be detected by XRD and TEM. Therefore, larger sizes calculated from XRD and TEM are not unexpected. If this stoichiometry is indeed applicable, it shows that titania also alters oxygen adsorption and only one surface monolayer of oxygen is formed on large nickel particles. Any error caused by an underestimation of the O_2 blank on Ni/TiO_2 would result in an underestimation of Ni particle size, and particle sizes would actually be larger than those calculated. This would increase the discrepancy of particle sizes calculated from O_2 adsorption if an O/Ni_s ratio of 2 is assumed, and would make an adsorption stoichiometry of 1 an even more appropriate choice.

One explanation of the lower hydrogen and CO coverages is activated adsorption caused by an SMSI effect attributable to the titania; however, the isobars determined in this study clearly show that activated adsorption is not the cause of reduced monolayer coverages at 300 K. For an adsorption process controlled only by thermodynamic considerations, the quantity of gas adsorbed is expected to fall continuously with increasing temperature as a consequence of the Clausius–Clapeyron equation applied to exothermic adsorption. Hydrogen adsorption on 6.8% Ni/SiO_2 exhibits this behavior and is in good agreement with the results of Schuit and Van Reijen (*35*), which have been plotted and compared directly elsewhere (*21*). The general behavior of 6.5% Ni/Al_2O_3 is similar although a shallow adsorption maximum may exist at 373 K. This may be a consequence of a slightly stronger interaction between nickel and alumina, which has been observed in previous studies (*8, 15, 36*). Hydrogen adsorption on 7.0% Ni/TiO_2 also exhibits a shallow maximum near 473 K, where the uptake is 40% higher than that at 300 K, and is indicative of some activated adsorption. *However, the most important result is that the additional uptake is very small and cannot account for the low H_2 uptakes at 300 K.*

The CO isobar shown in Fig. 2 for 7.0% Ni/TiO_2 apparently is the first reported for a nickel catalyst, presumably because of the potential problem of carbonyl formation. Although its shape is definitely unusual, activated adsorption is clearly not responsible for the lower CO uptakes because the maximum uptake occurs at the

lowest temperature. The shape is reproducible as shown by data obtained on two separate samples. The increase between 373 and 473 K may be due to a secondary process such as CO dissociation to alter surface coverage or to CO disproportionation to form surface carbon. Additional studies are required to explain this behavior. Regardless, surface coverage of CO at temperatures used for hydrogenation is only half the CO coverage at 300 K.

Regardless of the choice of the O/Ni_s ratio, H and CO coverages are clearly lower on TiO_2-supported nickel than on normal nickel surfaces. The relatively constant O/H values in Table 2 indicate an average hydrogen surface coverage less than 30% assuming an O/Ni_s ratio of 1, and a coverage slightly over 50% if a ratio of 2 is chosen. A trend exists for the O/CO ratio, with low values near 1 occurring for low loadings and high values near 4 existing for high loadings. This may be a consequence of the capability of small nickel crystallites, favored by low loadings, to form subcarbonyls (*8*).

The nature of the metal–support interaction which causes these changes in adsorption and catalytic properties is not well understood at this time. It may be primarily due to electron transfer (*37*) or to changes in crystallite morphology. Simple explanations such as nickel titanate formation do not seem appropriate because recent studies on Ni/TiO_2 have indicated a net electron donation to the nickel particles (*38*). Regardless, oxygen appears to be a satisfactory adsorbate for measuring nickel surface area in these Ni/TiO_2 systems, but the importance of slow admission rates of gas to the catalyst, which has been noted earlier (*18, 32*), must be emphasized.

SUMMARY AND CONCLUSIONS

This study has utilized chemisorption techniques, XRD, and TEM to provide evidence that SMSI behavior occurs in Ni/TiO_2 catalysts. Hydrogen and carbon monoxide monolayer coverages are suppressed on TiO_2-supported nickel whereas oxygen chemisorption stoichiometry appears to be near unity, a value normally found only for very highly dispersed nickel. As a consequence, carefully conducted oxygen adsorption experiments at room temperature can be utilized as an accurate method for measuring nickel surface area of titania-supported nickel catalysts, whereas H_2 and CO chemisorption does not provide accurate measurements. Good agreement among particle sizes determined by H_2, O_2, and CO chemisorption, XRD, and TEM was obtained for 6.8% Ni/SiO_2 and 6.5% Ni/Al_2O_3. For Ni/TiO_2 catalysts, however, excellent agreement existed only for sizes obtained from XRD, TEM, and O_2 chemisorption while particle sizes determined from CO and H_2 adsorption were far too large. This agreement implies that oxygen adsorption on TiO_2-supported nickel is limited to monolayer coverage.

Little or no activated H_2 adsorption was observed for Ni/SiO_2 and Ni/Al_2O_3 catalysts between 300 and 573 K. A small amount of activated H_2 adsorption occurred on Ni/TiO_2 but it cannot explain the low hydrogen saturation coverages at 300 K. Although the CO isobar had an unusual shape, the CO uptakes were highest at 300 K which clearly showed that the low CO coverages on TiO_2-supported nickel cannot be attributed to activated adsorption.

The lower electron density of nickel and the opacity of the crystalline titania particles increased the difficulty of distinguishing the nickel particles from titania using TEM. However, evidence of low-contrast, raft-like Ni particles was obtained although three-dimensional nickel particles were also observed. Increasing the nickel loading from 7.0 wt% to 12.3 wt% on titania had little effect on the Ni crystallite size distribution.

This study provides strong evidence that titania alters the adsorption behavior of nickel compared to unsupported nickel or nickel dispersed on silica or alumina. Titania-supported nickel exhibits unusually low

CO and H_2 monolayer coverages, a shift in the O/H ratio from 2 to 4, an apparent decrease in the O/Ni ratio from 2 to 1, and the possible presence of two-dimensional, raft-like crystallites. These results support the conclusion that SMSI behavior exists in Ni/TiO_2 catalyst systems.

ACKNOWLEDGMENT

This research was supported by Grant EG-77-S-02-4463 from the Division of Chemical Sciences, Office of Basic Energy Research, U.S. Department of Energy.

REFERENCES

1. Tauster, S. J., Fung, S. C., and Garten, R. L., *J. Amer. Chem. Soc.* **100,** 170 (1978).
2. Baker, R. T. K., Prestridge, E. B., and Garten, R. L., *J. Catal.* **56,** 390 (1979).
3. Baker, R. T. K., Prestridge, E. B., and Garten, R. L., *J. Catal.* **59,** 293 (1979).
4. Vannice, M. A., *in* "Symposium on Advances in Catalytic Chemistry," Snowbird, Utah, Oct. 3–5, 1979.
5. Vannice, M. A., and Garten, R. L., *J. Catal.* **56,** 236 (1979).
6. Garten, R. L., *J. Catal.* **43,** 18 (1976).
7. Palmer, M. B., Jr., and Vannice, M. A., *J. Chem. Technol. Biotechnol.* **30,** 205, (1980).
8. Bartholomew, C. H., and Pannell, R. B., *J. Catal.* **65,** 390 (1980).
9. Benson, J. E., and Boudart, M., *J. Catal.* **4,** 704 **65,** 390 (1980).
10. Wilson, G. R., and Hall, W. K., *J. Catal.* **17,** 190 (1970).
11. Yates, D. J. C., and Sinfelt, J. H., *J. Catal.* **8,** 348 (1967).
12. Bartholomew, C. H., and Farrauto, R. J., *J. Catal.* **45,** 41 (1976).
13. Thrower, P. A., personal communication (1979).
14. Toyoshima, I., and Somorjai, G. A., *Catal. Rev. Sci. Eng.* **19,** 105 (1979).
15. Mustard, D. G., and Bartholomew, C. H., submitted for publication.
16. Flynn, P. C., Wanke, S. E., and Turner, P. S., *J. Catal.* **33,** 233 (1974).
17. Van Hardeveld, R., and Van Montfoort, A., *Surface Sci.* **4,** 396 (1966).
18. Buyanova, N. E., Karnaukhov, A. P., Kefeli, L. M. Ratner, I. D., and Chernyavskaya, O. N., *Kinet. Katal.* **8,** 868 (1967).
19. Richardson, J. T., and Dubus, R. J., *J. Catal.* **54,** 207 (1978).
20. Shephard, R. E., *J. Catal.* **14,** 148 (1969).
21. Smith, J. S., M. S. thesis, The Pennsylvania State University, 1980.
22. Prestridge, E. B., Via, G. H., and Sinfelt, J. H., *J. Catal.* **50,** 115 (1977).
23. Yates, D. J. C., Murrell, L. L., and Prestridge, E. B., *J. Catal.* **57,** 41 (1979).
24. Treacy, M. M. J., and Howie, A., *J. Catal.* **63,** 265 (1980).
25. Anderson, J. R., "Structure of Metallic Catalysts," pp. 358–368 Academic Press, New York, 1975.
26. Vannice, M. A., and Garten, R. L., *J. Catal.* **66,** 242 (1980).
27. Criado, J. M., *React. Kinet. Catal. Lett.* **8,** 143 (1978).
28. Klemperer, D. F., and Stone, F. S., *Proc. Roy. Soc. London Ser. A* **243,** 375 (1958).
29. Brennan, D., Hayward, D. O., and Trapnell, B. M. W., *Proc. Roy. Soc. London Ser. A* **256,** 81 (1960).
30. Holloway, P. H., and Hudson, J. B., *Surface Sci.* **43,** 123 (1974).
31. Holloway, P. H., and Hudson, J. B., *Surface Sci.* **43,** 141 (1974).
32. Müller, J., *J. Catal.* **6,** 50 (1966).
33. Beeck, O., Smith, A. E., and Wheeler, H., *Proc. Roy. Soc. London Ser. A* **177,** 62 (1940).
34. Pannell, R. B., Chung, K. S., and Bartholomew, C. H., *J. Catal.* **46,** 340 (1977).
35. Schuit, G. C. A., and Van Reijen, L. L., *Advan. Catal.* **10,** 242 (1958).
36. Bartholomew, C. H., Pannell, R. B., and Butler, J. L., *J. Catal.* **65,** 335 (1980).
37. Tauster, S. J., Fung, S. C., Baker, R. T. K., and Horsley, J. A., *Science*, in press.
38. Kao, C. C., Tsai, S. C., Bahl, M. K., Chung, Y. W., and Lo, W. J., *Surface Sci.* **95,** 1 (1980).